

# Output-Feedback Model Predictive Control of Sewer Networks Through Moving Horizon Estimation

Bernat Joseph-Duran, Carlos Ocampo-Martinez, *Senior Member, IEEE*, and Gabriela Cembrano

**Abstract**—Based on a simplified control-oriented hybrid linear delayed model, *model predictive control* (MPC) of a sewer network designed to reduce pollution during heavy rain events is presented. The lack of measurements at many parts of the system to update the initial conditions of the *optimal control problems* (OCPs) leads to the need for estimation techniques. A simple modification of the OCP used in the MPC iterations allows to formulate a *state estimation problem* (SEP) to reconstruct the full system state from a few measurements. Results comparing the system performance under the MPC controller using full-state measurements and a *moving horizon estimation* (MHE) strategy solving a finite horizon SEP at each time instant are presented. Closed-loop simulations are performed by using a detailed physically-based model of the network as virtual reality.

## I. INTRODUCTION

Combined sewer networks carry both wastewater and storm-water together. During normal operation all the water is delivered to wastewater treatment plants (WWTP), where it is treated before being released to the receiving environment. However, during heavy rain events the network may become overloaded. In this situation, to prevent infrastructure damages, untreated water is released to the natural environment. To avoid these events, known as *combined sewer overflows* (CSO), the efficient management of the network infrastructure is of capital importance.

Real-time control (RTC) strategies taking advantage of rainfall forecasts and network measurements are regarded as the best option to compute control actions for the network regulation [1]. However, the physically-based model of open-channel flow describing the network dynamics involves the solution of a set of partial differential equations (the Saint-Venant equations, [2]) leading to prohibitive computational times in the case of mid- to large-scale networks. Simplified control-oriented models developed in the last few years allow for the computation of control actions in the available times while still providing sufficient accuracy [3], [4], [5], [6]. The use of these models in an MPC strategy allows also to take into account the system physical limits and to use rainfall forecasts to anticipate the future evolution of the system.

The main difference among the previously mentioned studies lies in the control model, since the MPC strategies are always based on minimization of the flows leading to pollution in the surrounding environment. Therefore, a comparative study of the performance these approaches is

out of the scope of this work since it would require to implement different models of the considered network. The MPC controller used in this work was already described in [15], [16] and shown to outperform the current static control approach. Here, the focus is on whether the lack of full state measurements affects the performance of the closed-loop system.

On the other hand, MPC requires full knowledge of the system variables to update the initial conditions of the *optimal control problems* (OCPs) solved at every time step. Due to the large-scale nature of sewer networks, full measurement is usually not available. To overcome this problem, observation/estimation techniques can be used to reconstruct the full network state from a few measurements.

Being the natural counterpart of MPC, the *moving horizon estimation* (MHE) strategy is based on solving a finite horizon *state estimation problem* (SEP) at each time instant, consisting of an optimization problem to minimize the difference between the measured outputs and those generated by the model. The ideas of MHE date back to the 90s, and its theoretical properties were developed in the years to follow for linear [7], nonlinear [8], [9] and hybrid systems [10], [11]. Unlike other classical observer and estimation techniques (e.g., Luenberger, Kalman filter) the MHE strategy can naturally handle system constraints and be applied to linear, nonlinear and hybrid systems. However, very few applications to water systems have been reported, with [12], [13] being the only ones known to the authors. In [13], the MHE strategy is used to estimate flows in a river system, much like in the present document, but based on a model leading to mid-scale smooth nonlinear optimization problems. Notice also that in the flow estimation problem the plant model is a set of partial differential equations, which prevents the use of error-based output MPC techniques [14].

In this work, a variation of the deadbeat observer presented in [10] based on 1-norm minimization is described and used as a SEP in a MHE strategy. The observed system state is then used as initial condition for an OCP to regulate a sewer network. Since the system model is a constrained linear hybrid model, both the SEP and the OCP result in *mixed integer linear programming* (MILP) problems. The main contribution of this paper is to couple both the MHE and MPC techniques in an output-feedback control strategy for a large-scale constrained mixed-integer problem: sewer network regulation. The performance of the overall control strategy is assessed by iteratively simulate the network using a detailed nonlinear physically-based model simulator, solve the SEP problem and solve the OCP. Results comparing this

All authors are with the Institut de Robòtica i Informàtica Industrial (CSIC-UPC), Carrer Llorens i Artigas, 4-6, 2a planta, 08028, Barcelona (Spain). Gabriela Cembrano is also with CETaqua Water Technology Center (Agbar-CSIC-UPC), Carretera d'Esplugues, 75, Cornellà, 07940, Barcelona (Spain). {bjoseph, cocampo, cembrano}@iri.upc.edu

strategy with full-state measurement are also provided, and show no significant performance loss.

The remainder of the paper is organized as follows: in Section II an overview of the sewer network model is presented, together with the general hybrid linear delayed system expression. The OCP and SEP problems based on the model are formulated in Sections III and IV. In Section V, the closed-loop simulation algorithm for the MPC/MHE strategy is presented together with results for a real case study. Finally, conclusions are presented in Section VI together with some future work research lines.

## II. HYBRID LINEAR DELAYED SEWER NETWORK MODEL

A *hybrid linear delayed model* has been chosen as the modeling framework for the sewer network description since it efficiently deals with three main aspects of the problem. Firstly, the presence of *delays* in the model is a common element in any water transportation model. Secondly, the *hybrid* approach allows to model the presence of overflows in the network, which only occur when a given flow is above a threshold value, thus according to a logical condition. Finally, the *linear* framework is specially suited for computational reasons since sewer networks are usually *large-scale* systems with a high number of variables.

The sewer network model used in this work consists of the following elements: flow model (including mass balance equations and flow equations), reservoir model, collector model, weir model, overflow and flood runoff model and rainfall-runoff model. The corresponding system variables are listed in Table I.

TABLE I  
SYSTEM VARIABLE NOTATION

| Description          | Symbol         | Units             | Indexing          |
|----------------------|----------------|-------------------|-------------------|
| Flow entering sewers | $q_i^{in}(t)$  | m <sup>3</sup> /s | $i = 1 \dots n_q$ |
| Flow leaving sewers  | $q_i^{out}(t)$ | m <sup>3</sup> /s | $i = 1 \dots n_q$ |
| Volume in tanks      | $v_i(t)$       | m <sup>3</sup>    | $i = 1 \dots n_v$ |
| Flow under gates     | $g_i(t)$       | m <sup>3</sup> /s | $i = 1 \dots n_g$ |
| Flow over weirs      | $w_i(t)$       | m <sup>3</sup> /s | $i = 1 \dots n_w$ |
| Overflows            | $f_i(t)$       | m <sup>3</sup> /s | $i = 1 \dots n_f$ |
| Flood runoff flow    | $qt_i(t)$      | m <sup>3</sup> /s | $i = 1 \dots n_f$ |
| Overflow volume      | $vt_i(t)$      | m <sup>3</sup> /s | $i = 1 \dots n_f$ |
| Rain inflow          | $c_i(t)$       | m <sup>3</sup> /s | $i = 1 \dots n_c$ |

The main system equations are the flow equations, relating the in- and outflow at each network sewer, which take into account the transport delay and flow attenuation. The flow downstream of each sewer is computed by means of a convex combination of the upstream flows at two previous time steps. Hence, for each sewer  $i = 1 \dots n_q$

$$q_i^{out}(t) = a_i q_i^{in}(t - t_i) + (1 - a_i) q_i^{in}(t - t_i - 1), \quad (1)$$

where  $t \in \mathbb{Z}$  is the discrete time variable,  $a_i \in (0, 1]$  are the coefficients of the convex combination and  $t_i$  the sewer delay [16].

Reservoirs are modeled with the usual discrete-time mass balance equations. The collector model describes sewers of

big dimensions which can be used for in-line water retention. They are modeled as a series of reservoirs each one adding a one time step delay to the flow through the collector. The last reservoir outflow is regulated with a sluice gate.

Weir flows are described by means of maximum functions:

$$w(t) = \max\{0, a_w(z_w(t) - q_w^{max})\}, \quad (2)$$

where  $w(t)$  is the flow over the weir,  $z_w(t)$  is the inflow to the junction where the weir is attached,  $q_w^{max}$  is the maximum inflow before water starts flowing through the spillway and  $a_w$  is a parameter introduced for calibration purposes. Overflows and flood runoff flows are also described in a similar way using piecewise linear functions. These functions are reformulated into linear inequalities by means of the *mixed logical dynamic* (MLD) systems approach [17]. To this end, binary variables need to be defined, turning the system into a *hybrid system*. Please, refer to [16] for a complete description of the model with calibration and validation results.

An important feature of the control model and the plant model equations is that they are all mass-conservative. Therefore, since the amount of water entering the network in a rain event is finite, stability of the closed-loop system can be guaranteed.

Putting all the equations and MLD inequalities together, the system can be written in the following compact form, that will be useful for the OCP and SEP formulation:

$$\begin{aligned} \sum_{i=0}^T M_i X(t-i) &= m(t), \\ \sum_{i=0}^T N_i X(t-i) &\leq n(t), \end{aligned} \quad (3)$$

where

$$X(t-i) = (x_1(t-i), \dots, x_n(t-i))^T, \quad i = 0, \dots, T, \quad (4)$$

with  $x_j(t-i) \in \mathbb{R}$  for a subset of indices  $j \in \mathcal{C} \subset \{1, \dots, n\}$  and  $x_j(t-i) \in \{0, 1\}$  for a subset of indices  $j \in \mathcal{B} \subset \{1, \dots, n\}$ . Index sets  $\mathcal{C}$  and  $\mathcal{B}$  are such that  $\mathcal{C} \cap \mathcal{B} = \emptyset$  and  $\mathcal{C} \cup \mathcal{B} = \{1, \dots, n\}$ .  $M_i$ ,  $i = 0, \dots, T$ , and  $N_i$ ,  $i = 0, \dots, T$ , where  $T$  is the maximum system delay, are matrices of appropriate dimensions. Binary variables can have a direct physical meaning but more commonly arise in the MLD reformulation of the model equations.

In system (3), the set of equalities contains the network junction mass balance equations, the delayed transport equations and the tank volume equations. The set of inequalities corresponds to constraints arising from the MLD description of the piecewise equations describing both the weir flow and overflow variables (see [18] for details).

Vectors  $X(t-i)$ ,  $i = 0, \dots, T$ , include all system variables, making no distinction whether they are either state, input or output variables. The influence of the rain inflows (disturbances) at any time instant is included in vectors  $m(t)$  and  $n(t)$ .

### III. OPTIMAL CONTROL PROBLEM

The formulation of the OCP associated with model (3) was already described in [15]. It is based on imposing equations and inequalities (3) from time steps  $t+1$  to  $t+H$ , where  $H$  is called the prediction horizon, as constraints of an optimization problem aiming to minimize a performance index. The general form of the OCP is as follows:

$$\begin{aligned} \min_{\mathcal{X}(t)} \quad & J(\mathcal{X}(t)) = c^\top \mathcal{X}(t), \\ \text{s.t.} \quad & \mathcal{M}_1 \mathcal{X}(t) = \mathcal{M}_2 \mathcal{X}_0(t) + \mathcal{M}_3(t), \\ & \mathcal{N}_1 \mathcal{X}(t) \leq \mathcal{N}_2 \mathcal{X}_0(t) + \mathcal{N}_3(t), \\ & A_{eq} \mathcal{X}(t) = b_{eq}(t), \\ & A_{ineq} \mathcal{X}(t) \leq b_{ineq}(t), \end{aligned} \quad \text{OCP}(t)$$

where  $\mathcal{M}_i$  and  $\mathcal{N}_i$  are block matrices build from the matrices of system (3) (see [15] for the precise block structure) and

$$\begin{aligned} \mathcal{X}(t) &= (X(t+H)^\top, \dots, X(t+1)^\top)^\top, \\ \mathcal{X}_0(t) &= (\tilde{X}(t)^\top, \dots, \tilde{X}(t-T+1)^\top)^\top, \end{aligned} \quad (5)$$

contain, respectively, the problem unknowns along the prediction horizon and the values of the system variables at the current and previous time instants. The latter can either be measured in the case of full-state measurement or provided by means of some estimation technique as described in the next section.

The choice of vector  $c$  in the OCP objective function depends on the control objectives. In this work the objective is to minimize pollution, thus  $c$  is defined as  $c = 10 \cdot c_{COF} + c_{OF} + c_{CSO} - 10^{-1} \cdot c_{WWTP}$ , where  $c_{COF}$ ,  $c_{OF}$ ,  $c_{CSO}$ , and  $c_{WWTP}$ , are 0-1 vectors selecting the collector overflow variables (COF), the overflow variables (OF), the flows to the receiving environment (CSO) and the flows to the WWTP (with negative weight to be maximized), respectively. The choice of the weight values is discussed in [16].

Notice, also, the addition of further equalities  $A_{eq} \mathcal{X}(t) = b_{eq}(t)$ , and inequalities  $A_{ineq} \mathcal{X}(t) \leq b_{ineq}(t)$ . These are any other additional constraints to be added to the system to improve its behavior. Typical ones include bounds on the controlled variables due to physical limits and bounds on its variation rates, to ensure smooth control actions.

The only physical constraints in the model are the tank volumes which, are always regulated by gates, thus avoiding infeasibilities in the associated optimization problem. Bounds on all the other variables are added to speed up the optimization. Lower bounds are all set to zero and values for upper bounds are obtained from the rain inflow values (disturbances) corresponding to several real-rain events. Since the model equations are all mass balances and transport equations, the feasibility of the problems is guaranteed unless some upper bound is violated, which is never the case, since the considered upper bound values have all been increased to be above the ones resulting from the heaviest rain episodes. The same reasoning applies to the SEP described in the next section.

### IV. STATE ESTIMATION PROBLEM

State estimation problems aim to reconstruct the full system state out of a few output measurements. To this end, the difference between the system measurements and the outputs generated by the estimator model is minimized along a finite past horizon by means of an optimization problem. Due to plant-model mismatch, generally, no sequence of model generated outputs can meet exactly the measured values. To take into account this fact two formulations of the SEP are usually applied: in the first one involves adding slack/noise variables to each system dynamic and output equation and minimizing these variables while forcing the model outputs to be equal to the measured ones [7], [10], [11]. The second formulation is a direct minimization of the norm of the difference between the model generated outputs and the measured ones [8], [12], [13]. The former appears to be more appealing for theoretical purposes since it explicitly deals with the slack/noise variables. For simplicity of the implementation latter formulation will be used in the following.

The state estimation problem is analogous to the OCP one but the system dynamics and inequality constraints are enforced for the past states rather than for the future ones:

$$\begin{aligned} \sum_{i=0}^T M_i X_o(t-i+k) &= m(t+k), \\ \sum_{i=0}^T N_i X_o(t-i+k) &\leq n(t+k), \\ k &= -H_o + T + 1, \dots, 0, \end{aligned} \quad (7)$$

where  $H_o$  is the number of past instant measured variables that will be used in the problem. The state estimation problem variable is then defined as:

$$\mathcal{X}_o(t) = (X_o(t)^\top, \dots, X_o(t-H_o+1)^\top)^\top, \quad (8)$$

Vectors  $X_o(t)$  are defined in the same way as  $X(t)$ , but a different notation is used to distinguish the variables of the SEP and OCP in the closed-loop algorithm.

To express the constraints in matrix form, the following matrices are defined:

$$\begin{aligned} \mathcal{M}_1^o &= \left( \begin{array}{cccc} M_0 & M_1 & \dots & M_{T-1} & M_T \\ & \ddots & \ddots & \ddots & \ddots \\ & & M_0 & M_1 & \dots & M_{T-1} & M_T \end{array} \right) \Bigg\}^{H_o-T}_{\text{blocks}}, \\ \mathcal{M}_2^o(t) &= (m(t)^\top, \dots, m(t-H_o+1)^\top)^\top, \end{aligned} \quad (10)$$

with analogous expressions for  $\mathcal{N}_1^o$  and  $\mathcal{N}_2^o$ . Hence, the state estimation problem can be written as:

$$\begin{aligned} \min_{\{X_o(t), \varepsilon_y, \varepsilon_u\}} \quad & \mathbf{1}^\top \varepsilon_y + \mathbf{1}^\top \varepsilon_u, \\ \text{s.t.} \quad & \mathcal{M}_1^o(t) \mathcal{X}_o(t) = \mathcal{M}_2^o(t), \\ & \mathcal{N}_1^o(t) \mathcal{X}_o(t) \leq \mathcal{N}_2^o(t), \\ & -\varepsilon_y \leq \Pi_y \mathcal{X}_o(t) - \tilde{\mathcal{Y}} \leq \varepsilon_y \\ & -\varepsilon_u \leq \Pi_u \mathcal{X}_o(t) - \tilde{\mathcal{U}} \leq \varepsilon_u \\ & A_{eq}^o \mathcal{X}_o(t) = b_{eq}^o(t), \\ & A_{ineq}^o \mathcal{X}_o(t) \leq b_{ineq}^o(t), \end{aligned} \quad \text{SEP}(t)$$

where

$$\tilde{\mathcal{Y}}(t) = (\tilde{Y}(t)^\top, \dots, \tilde{Y}(t - H_\mathcal{O} + 1)^\top)^\top, \quad (11)$$

$$\tilde{\mathcal{U}}(t) = (\tilde{U}(t)^\top, \dots, \tilde{U}(t - H_\mathcal{O} + 1)^\top)^\top, \quad (12)$$

are the measured outputs and inputs at previous time steps. Notice that, with the present formulation, the output vector  $\mathcal{Y}$  and the input vector  $\mathcal{U}$  (resp.  $Y$  and  $U$ ) are subsets of vector  $\mathcal{X}_\mathcal{O}$  (resp.  $X_\mathcal{O}$ ), therefore they can be expressed by means of 0-1 projection vectors  $\Pi_\mathcal{Y}$  and  $\Pi_\mathcal{U}$  such that

$$\Pi_\mathcal{Y} \mathcal{X}_\mathcal{O}(t) = (Y(t)^\top, \dots, Y(t - H_\mathcal{O} + 1)^\top)^\top, \quad (13)$$

$$\Pi_\mathcal{U} \mathcal{X}_\mathcal{O}(t) = (U(t)^\top, \dots, U(t - H_\mathcal{O} + 1)^\top)^\top, \quad (14)$$

Variables  $\varepsilon_\mathcal{Y}$  and  $\varepsilon_\mathcal{U}$  are auxiliary variables used to reformulate the minimization of the 1-norms  $\|\Pi_\mathcal{Y} \mathcal{X}_\mathcal{O}(t) - \tilde{\mathcal{Y}}\|_1$  and  $\|\Pi_\mathcal{U} \mathcal{X}_\mathcal{O}(t) - \tilde{\mathcal{U}}\|_1$  as a MILP [19]. The inequalities involving  $\varepsilon_\mathcal{Y}$  and  $\varepsilon_\mathcal{U}$  already imply that these variables should take positive values ( $-\varepsilon \leq \varepsilon \Rightarrow \varepsilon \geq 0$ ).

As in the OCP, further equalities  $A_{eq}^\mathcal{O} \mathcal{X}(t) = b_{eq}^\mathcal{O}(t)$ , and inequalities  $A_{ineq}^\mathcal{O} \mathcal{X}(t) \leq b_{ineq}^\mathcal{O}(t)$ , are added to take into account additional constraints other than the system dynamics.

Notice that, in (7), the system equations are only enforced for the last  $H_\mathcal{O} - T$  time instants:  $X_\mathcal{O}(t)$  to  $X_\mathcal{O}(t - H_\mathcal{O} + T + 1)$ . Therefore,  $H_\mathcal{O} \geq 2T$  is assumed in order that the system equations are enforced for the variables needed to be used as initial conditions for the OCP. The rest of variables at the first  $T$  time instants  $t - H_\mathcal{O} + T, \dots, t - H_\mathcal{O} + 1$ , are left free. In this way the estimated inputs and outputs at these times, will take exactly the same values as the measured ones as a result of the optimization contributing, through the delays in the equations, to a better estimation of the rest of the variables at later time instants.

## V. OUTPUT-FEEDBACK CLOSED-LOOP ALGORITHM AND RESULTS

The MPC technique consists of solving a finite horizon OCP at each time step and then applying to the system the part of the solution corresponding to the first time step before measuring the system state again and repeating the procedure. The initial value for the model in each OCP is obtained from the last measurements of the system, thus providing the state feedback. Similarly, the MHE strategy consists of solving a finite horizon SEP at each time step to estimate the system state. Again, the last measurements of the system are used as the reference for the SEP, to which the estimator states would ideally converge. When using both techniques together, the state variables estimated by the SEP are used as initial conditions for the OCP.

To test the output-feedback MPC/MHE controller the physically-based model simulator MOUSE [20] has been used as a virtual reality. MOUSE solves the complete Saint-Venant equations and also simulates local PID controllers for gate flow regulation. The modeling and output-feedback control strategy have been applied to the real case study of a part of the Barcelona sewer network, whose simplified connection scheme is shown in Figure 1. The implementation

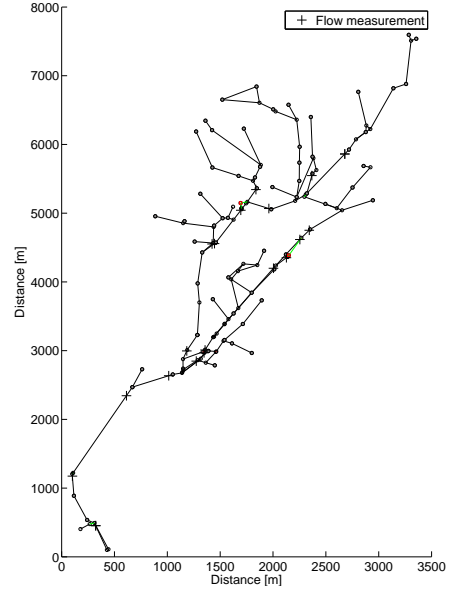


Fig. 1. Diagram of the simplified case-study network.

of the network model in MOUSE together with all the needed parameters have been provided by CLABSA (CLavegueram de Barcelona S.A.), the company responsible of the network management.

The control model for the studied network consists of  $n_v = 2$  tanks,  $n_q = 145$  sewers,  $n_w = 3$  weirs,  $n_f = 11$  overflows,  $n_g = 10$  gates,  $n_c = 1$  collector and  $n_r = 68$  rain inflows. The sampling time has been chosen of  $\Delta t = 1$  min with a maximum delay in sewers of  $T = 6$  min. For the estimation problem, flows at 20 sewers ( $Y(t)$ ) are measured together with those at the  $n_g = 10$  regulated gates ( $U(t)$ ). The location of the flow measurements, shown in Figure 1, is based on real data also provided by CLABSA.

In this work, the model predictive controller is used as an upper level controller that computes optimal gate flow values. These values are then used as set-points for local PID controllers that regulate the gate positions to achieve the desired flows. Once the set-points for the local controllers at the network gates are updated, some time is needed for the gates to move and reach the desired flow values. Therefore, the SEP and OCP are solved every five time steps (that is, five minutes) instead of every time step and the PID set-points are kept constant during this time. In a real application, this time would also include the time needed for data acquisition from a SCADA system and the time needed to solve the SEP and the OCP. The fact that the PID set-points can only change every five minutes is taken into account in the OCP by means of additional constraints forcing the gate flows to remain constant during intervals of five time steps.

Also as a consequence of the predictive controller acting as an upper level controller delivering set-points to local controllers, the manipulated variables  $U(t)$  may not achieve exactly the set-point values and therefore measures of these variables are used in the SEP to estimate the system state.

The SEP and OCP are integrated in the output-feedback MPC/MHE closed-loop algorithm as follows. At time step  $t$ :

- Measure system outputs and inputs:  $\tilde{\mathcal{Y}}(t), \tilde{\mathcal{U}}(t)$
- Solve SEP( $t$ ) to compute  $\mathcal{X}_o^*(t)$
- Set OCP( $t$ ) initial conditions as

$$\mathcal{X}_0(t) := (X_o^*(t)^\top, \dots, X_o^*(t - T + 1)^\top)^\top$$

- Solve OCP( $t$ ) to compute  $\mathcal{X}^*(t)$
- Set physically-based model simulator PID set-points to

$$U_{PID} = U^*(t)$$

- Run five minutes simulation of the physically-based model
- Set  $t := t + 5$

Here, variables with a star upper index indicate that they are the solution of the corresponding optimization problem. Figure 2 shows a diagram of the process.

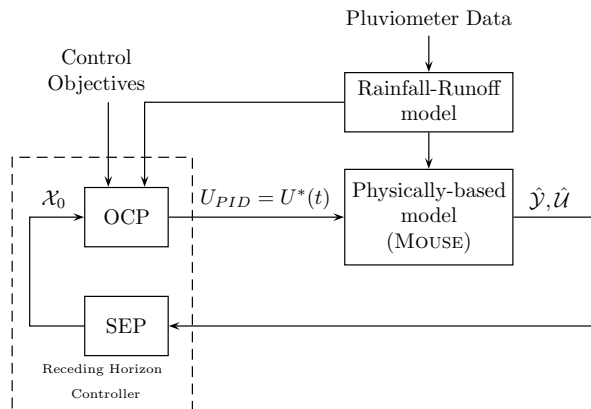


Fig. 2. Block diagram of the RHC strategy in closed-loop simulation.

The OCPs are solved with a prediction horizon of  $H = 40$  time steps, which is the network's concentration time, that is, the time needed for water to travel from the uppermost part of the network to its downstream end. For the SEPs a horizon of  $H_o = 15$  time steps has been chosen.

Table II shows the results of the closed-loop output-feedback simulations for four real-rain events. As mentioned before, the control objectives for this simulations are to minimize urban flooding (overflows), minimize CSOs and maximize WWTP usage. It can be noticed that no relevant performance loss is obtained when using the MHE strategy compared with the full-state measurement (FSM) case. In some cases there is even a reduction of the CSO objective. This is due to the fact that MPC, although based on solving optimal control problems, is not optimal along the whole simulation time. This, together with the fact that the solution of the OCP is not unique, causes the overall solution to be affected by the decisions made at each time step leading in some cases to some performance loss.

It can also be noticed that the overflow volume is identical in three of the scenarios. This is because in these scenarios overflows downstream of the flow regulation elements are completely avoided. Then, overflows upstream of those regulation elements take the same values no matter which control or estimation strategy is used.

To assess the SEP accuracy at estimating the system states, the following error index for the flow variables has been

TABLE II  
RECEDING HORIZON RESULTS

| Episode    | Measurements | Overflow<br>[ $\times 10^3 \text{m}^3$ ] | CSO<br>[ $\times 10^3 \text{m}^3$ ] | WWTP<br>[ $\times 10^3 \text{m}^3$ ] |
|------------|--------------|--|-------------------------------------|--------------------------------------|
| 17-09-2002 | MHE          | 0.1488                                   | 3.8412                              | 74.7820                              |
|            | FSM          | 0.1578                                   | 8.9983                              | 75.0095                              |
| 09-10-2002 | MHE          | 1.0833                                   | 340.7905                            | 88.8712                              |
|            | FSM          | 1.0075                                   | 341.6726                            | 88.5412                              |
| 15-08-2006 | MHE          | 0.2501                                   | 4.8475                              | 53.0944                              |
|            | FSM          | 0.2501                                   | 4.5822                              | 53.1046                              |
| 30-07-2011 | MHE          | 0.7470                                   | 40.3150                             | 51.9380                              |
|            | FSM          | 0.7470                                   | 39.0140                             | 51.7179                              |

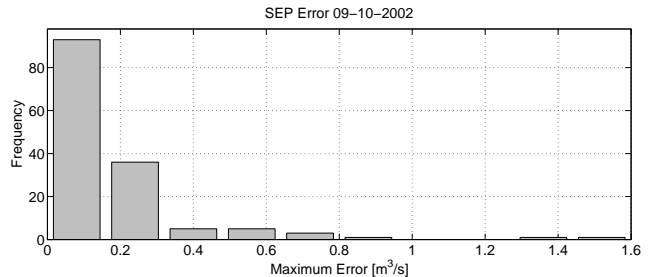


Fig. 3. Histogram of the maximum errors in the  $n_l = 145$  sewers for rain event 09-10-2002.

used:

$$e_i(t) = \max_{\tau=5t-T+1, \dots, 5t} |q_i^o(\tau) - \tilde{q}_i(\tau)|, \quad i = 1, \dots, n_l. \quad (15)$$

That is, for each SEP, the maximum deviation between the observed flow  $q_i^o$  and the real one  $\tilde{q}_i$  (as given by MOUSE) along the  $T$  time steps used to initialize the OCP. Figure 3 shows the distribution of the maximum error

$$\max_{t=1, \dots, t_s} e_i(t), \quad i = 1, \dots, n_l, \quad (16)$$

where  $t_s$  is the number of SEPs solved for rain event 09-10-2002. Convergence of the estimated values towards the measured ones is shown in Figure 4.

Real-time control requirements regarding computation times are also met. Table III shows the mean and maximum computation times for both the OCP and SEP for each of the simulated rain scenarios and Table IV shows the corresponding number of variables and constraints. The 60 seconds maximum times for scenarios 1 and 2 are due to a maximum time limit enforced in the optimizer settings. The time limit is reached three times for scenarios 1 and 2. In all the cases, the solver already reached a feasible sub-optimal solution with an objective value deviation from the optimal one of at most 1.11% (see MIP relative gap, [21]), which could be used to continue with the RTC iterations.

All optimization problems were solved using CPLEX v12.5 [21] MILP solver with standard settings, available through the IBM Academic Initiative, on a machine with an Intel Core 2 Duo CPU with 3.33 GHz and 8 GB RAM. Warm starting of each problem using the part of solution of the previous one corresponding to the overlapping time steps has been used to speed-up the computations.

TABLE III  
COMPUTATIONAL TIMES FOR THE OCP AND SEP

| Episode    | Mean OCP<br>Time [s] | Max OCP<br>Time [s] | Mean SEP<br>Time [s] | Max SEP<br>Time [s] |
|------------|----------------------|---------------------|----------------------|---------------------|
| 17-09-2002 | 0.52                 | 1.84                | 4.77                 | 60.01               |
| 09-10-2002 | 0.62                 | 3.23                | 4.44                 | 60.03               |
| 15-08-2006 | 0.49                 | 3.33                | 2.81                 | 36.47               |
| 30-07-2011 | 0.45                 | 2.20                | 3.03                 | 51.25               |

TABLE IV  
NUMBER OF VARIABLES AND CONSTRAINTS FOR THE OCP AND SEP.

|     | Continuous<br>Variables | Binary<br>Variables | Equality<br>Constraints | Inequality<br>Constraints |
|-----|-------------------------|---------------------|-------------------------|---------------------------|
| OCP | 8520                    | 1040                | 7440                    | 7240                      |
| SEP | 3645                    | 390                 | 1780                    | 2510                      |

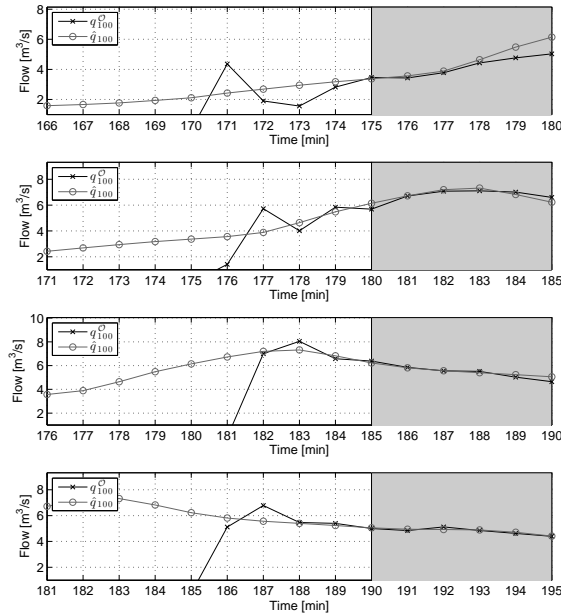


Fig. 4. Successive estimations of  $q_{100}$  for rain scenario 09-10-2002. The shaded area corresponds to the  $T$  time steps used for the OCP initial conditions and for the error calculation.

## VI. CONCLUSIONS AND FUTURE WORK

Based on a general hybrid linear delayed model of a sewer network, simple matrix-based procedures to formulate finite horizon optimal control problems (OCP) and state estimation problems (SEP) have been presented. Both problems are integrated into an output-feedback receding horizon control strategy to minimize pollution in the sewer network in presence of heavy rain events. Model predictive control (MPC) is used to compute optimal flows at each time step. To provide the initial conditions for the OCP solved in each MPC iteration, moving horizon estimation (MHE) is used to estimate the network flows using the latest system measurements. Closed-loop results using a detailed physically-based model simulator show that no significant performance loss is obtained using the MHE strategy compared with full-state measurement. The real-time control requirements regarding computation times, accuracy and performance are met.

Future research regarding estimation in sewer networks

should be focussed in developing flow-level relations to be able to use limnimeter measurements (i.e. water level measurements) in the estate estimation problem, aside from the flow-meter measurements used in this work.

## ACKNOWLEDGMENTS

This work has been partially funded by the research project ECOCIS (DPI-2013-48243-C2-1-R). The authors are especially grateful for the collaboration of the CLABSA staff in providing the test case, data and expert guidance.

## REFERENCES

- [1] M. Schütze, A. Campisano, H. Colas, W. Schilling, and P. Vanrolleghem, “Real time control of urban wastewater systems - where do we stand today?”, *Journal of Hydrology*, vol. 299, no. 3-4, pp. 335-348, 2004.
- [2] X. Litrico and V. Fromion, *Modelling and Control of Hydrosystems*. London: Springer, 2009.
- [3] M. Gelormino and N. Ricker, “Model-predictive control of a combined sewer system”, *Int. J. Control*, vol. 59, no. 3, pp. 793-816, 1994.
- [4] M. Marinaki and M. Papageorgiou, *Optimal Real-time Control of Sewer Networks*. London: Springer, 2005.
- [5] V. Puig, G. Cembrano, J. Romera, J. Quevedo, B. Aznar, G. Ramón, and J. Cabot, “Predictive optimal control of sewer networks using CORAL tool: application to Riera Blanca catchment in Barcelona”, *Water Science and Technology*, vol. 60, no. 4, pp. 869-878, 2009.
- [6] C. Ocampo-Martínez, V. Puig, G. Cembrano, and J. Quevedo, “Application of predictive control strategies to the management of complex networks in the urban water cycle”, *IEEE Control Systems*, vol. 33, no. 1, pp. 15-41, 2013.
- [7] C. Rao, J. Rawlings, and J. Lee, “Constrained linear state estimation—a moving horizon approach”, *Automatica*, vol. 37, pp. 1619-1628, 2001.
- [8] H. Michalska and D. Mayne, “Moving horizon observers and observer based control”, *IEEE Trans. Automat. Contr.*, vol. 40, no. 6, pp. 995-1006, 1995.
- [9] C. Rao, J. Rawlings, and D. Mayne, “Constrained state estimation for nonlinear discrete-time systems: stability and moving horizon approximations”, *IEEE Trans. Automat. Contr.*, vol. 48, no. 2, pp. 246-258, 2003.
- [10] A. Bemporad, G. Ferrari-Trecate, and M. Morari, “Observability and controllability of piecewise affine and hybrid systems”, *IEEE Trans. Automat. Contr.*, vol. 45, no. 10, pp. 1864-1876, 2000.
- [11] G. Ferrari-Trecate, D. Mignone, and M. Morari, “Moving horizon estimation for hybrid systems”, *IEEE Trans. Automat. Contr.*, vol. 47, no. 10, pp. 1663-1676, 2002.
- [12] J. Busch, P. Köhl, J. Schölder, H. Bock, and W. Marquardt, “State estimation for large-scale wastewater treatment plants”, *Water Research*, vol. 47, no. 13, pp. 4774-4787, 2013.
- [13] M. Breckpot, T. Blanco Barjas, and B. De Moor, “Flood control of rivers with nonlinear model predictive control and moving horizon estimation”, in *IEEE Conference on Decision and Control*, (Atlanta, USA), pp. 6107-6112, 2010.
- [14] J. Rawlings and D. Mayne, *Model Predictive Control: Theory and Design*. Madison: Nob Hill Publishing, 2009.
- [15] B. Joseph-Duran, C. Ocampo-Martínez, and G. Cembrano, “Receding horizon control of hybrid linear delayed systems: Application to sewer networks”, in *IEEE Conference on Decision and Control*, (Florence, Italy), pp. 2257-2262, 2013.
- [16] B. Joseph-Duran, C. Ocampo-Martínez, and G. Cembrano, “Hybrid modeling and receding horizon control of sewer networks”, *Water Resources Research*, 2014. DOI: 10.1002/2013WR015119.
- [17] A. Bemporad and M. Morari, “Control of systems integrating logic, dynamics, and constraints”, *Automatica*, vol. 35, no. 3, pp. 407-427, 1999.
- [18] B. Joseph-Duran, C. Ocampo-Martínez, and G. Cembrano, “Hybrid Linear Sewer Network Modeling”, Tech. Rep. IRI-TR-09-07, Institut de Robòtica i Informàtica Industrial, CSIC-UPC, 2013.
- [19] S. Boyd and L. Vandenberghe, *Convex Optimization*. Cambridge: Cambridge University Press, 2004.
- [20] MOUSE, *MOUSE User Guide*. DHI Software, 2007.
- [21] CPLEX™, *version 12.5 (2012)*. Sunnyvale, California: IBM ILOG, 2011.